Structural and UV-Vis absorption studies of Alkaline Earth Zinc Bismuth Borate Glasses Doped with Eu^{3+} ions

Ramesh Boda, G.Srinivas, D.Komaraiah, Md. Shareefuddin, M.N. Chary, R.Sayanna

Department of physics, Osmania University, Hyderabad-500007, Telangana, India.

Abstract : Glasses with the composition xCaO-15ZnO- 20Bi$_2$O$_3$- (64−x) B$_2$O$_3$- 1EuO [where x= 0, 5, 10, 15, 20 mol %] were prepared by the conventional melt quenching technique. X-ray diffraction studies, the differential scanning calorimetry (DSC), density of the samples were carried out. Molar volume was calculated from the density data, and the physical properties were calculated using density, refractive index. The optical absorption spectra in UV-Vis region were recorded in the wave length range 200-1000nm. Cut-off wavelength, direct, indirect band gap, Urbach energy, Molar refraction (R$_m$), Molar electronic polarizability (α_m), reflection loss and refractive index values were evaluated from absorbance data The structural changes in the boron and bismuth co-ordination with incorporation of alkaline earth oxide variations and rear earth (EuO) doping were investigated by FT-IR spectroscopic techniques.

Keywords - *Bismuth borate glass, XRD, UV, Density, Molar volume, refractive index, FTIR.*

I. INTRODUCTION

Glasses containing Bi$_2$O$_3$ have attracted considerable attention because of their wide applications in the field of glass-ceramics, thermal and mechanical sensors, reflecting windows, radiation shielding. They can be used as layers for optical and opto-electronic devices [1, 2]. Bismuthate glasses containing alkali oxide act as ionic conductors and possess high conductivity compared to other heavy metal oxide glasses. Among different glass matrices, scientific interest on bismuth borate glasses is attributed to their favorable properties such as rigid physical and chemical stability[1], high refractive index, extensive glass formation range, long infrared cutoff and large third order nonlinear optical susceptibility[7-10], low melting temperature[7,8], high density and high infrared transparency.

In the present system alkaline earth zinc bismuth borate (ZCB) glasses doped with Europium oxide, the oxides such as Bi$_2$O$_3$ are added to get good refractive index for using it in enhancement of other optical properties. ZnO could be found as the network modifiers(NWM), the oxygen becomes non-bridging when the divalent cation like zinc are incorporated in the glass network with relatively large composition range[7,8] and B$_2$O$_3$ can be used as the network former (NWF) and is contained in most of the important commercial glasses.

II. MATERIALS AND METHODS

Glass preparation: Reagent grade H$_3$BO$_3$, Bi$_2$O$_3$, ZnO and CaO with Eu$_2$O$_3$ as the dopant were used as the starting materials for preparing the glasses, the raw materials in the powder form were mixed using a mortar and pestle. Each mixture was put in muffle furnace melted in a porcelain crucible at 1000°C for 3–4 hour in air. The glass melts were stirred occasionally to achieve good homogeneity. The highly viscous melt was cast in to a cylindrically shaped mould of stainless steel. The glass produced was annealed at 200°C in a second furnace for 2 hr after which the furnace was switched off and the glass was allowed to cool gradually for 2 hrs.

The X-Ray diffractograms were recorded at room temperature with 0.02/sec scanning rate in the range (100-900) using the Philips X-Ray diffractometer with Kα tube target and nickel filter operated at 40 kV, 30mA.

All the x-ray diffractograms were recorded at room temperature. The peak free x-ray diffractograms confirmed [fig.1] the amorphous nature of the prepared glass samples.

The densities of these glass samples were determined at room temperature by the Archimedes principle using xylene as an immersion liquid.

The differential scanning calorimetry (DSC) thermograms were recorded using DSC Q20 V24.10 build 122 Instrument, at the rate of 10.00 °C/min,

The infrared transmittance spectra of the glass samples were recorded at room temperature by using Perkin Elmer Frontier FTIR in the mid-IR range (250-4000cm^{-1}) KBr pallet technique was used to record the IR spectra the sample was powdered with 0.3g of KBr in the ratio 2:100 and put in to a 13mm dye and passed with a pressure of 7-10 ton using hydraulic press to obtain transparent pallets of approximate 1mm thickness. The spectra of these pallets were then recorded by using universal sample holder with the resolution of 4 cm-1 and

16 scans per sample. The background removal and baseline correction was done with the help of spectrum 10 software.

The optical absorption spectra of the polished samples (optical path length or thickness 2.00mm) were recorded at room temperature using Analytical Technologies Limited (Philip halogen, deuterium lamp(200H), model: Spectro UV 2092) in the range 200–1000nm.

III.   RESULTS AND DISCUSSION

3.1. Physical properties

The density (ρ) values were estimated using the following formula:

$$\rho = \frac{w}{w - w_1} \times \rho_x$$

where w is the weight of the glass sample in air, w_1 is the weight of the glass sample when immersed in xylene of density (ρ_x) 0.865gm/cm^3.

The density verses mol% of CaO graph (fig.11) gave a non linear relation and the molar volume was calculated from the density data, using the formula

$$V = \frac{M}{\rho}$$ where M = average molecular weight, ρ=density.

The molar volume verses mol% of CaO graph (fig.11) shows a non linear relation.

The concentration of the rare earth doped ion was calculated using the following formula

$$N_i = \frac{mol\%. of \, dopent \, X \, Na \, X \, Density}{Avg. molecular. wt.}$$

The polaron radius of the atoms are calculated using the fallowing formula [7-9]

$$R_p = \frac{1}{2} \left(\frac{\pi}{6N_i} \right)^{\frac{1}{3}} A^0$$

where N_i is concentration of rear earth ions.

The inter molecular distance was calculated using the fallowing formula [7]

$$R_i = \left(\frac{1}{N_i} \right)^{\frac{1}{3}} A^0$$

where N_i is concentration of rare earth ions.

The field strength is calculated from the fallowing formula [7, 8]

$$(f) = \frac{Z}{R_p^2} \, cm^{-2}$$

where Rp is polaron radius and Z is oxidation number.

3.2. The DSC

the values of glass transition temperatures (table.1) are found to be around 447 to 472 centigrade's from which the glassy nature of samples is confirmed, as the mole percentage of calcium is increasing the transition temperature is decreasing (Fig.10).

3.3.1. Optical absorption

The Optical absorption spectra of the glass composition $xCaO-15ZnO- 20Bi_2O_3- (64-x) B_2O_3- 1EuO$ are shown in frg.2. in the optical absorption spectra transitions are assigned. It is clear from the fig.3 that the absorption edges were not sharp which is an indication of amorphous nature of the glass samples. The absorption coefficient, α (υ) were determined near the absorption edge of different photon energies for all the glasses using the relation [1, 3];

$$\alpha \, (\upsilon) = 2.303 \frac{A}{d}$$

where 'A' is the absorbance and'd' is the thickness of the sample. Davis and Mott proposed the following relation for amorphous materials where the absorption co-efficient α (υ) is a function of photon energy (hυ) for direct and indirect transitions [1, 7].

$$(\alpha h\upsilon)= B^2 (h\upsilon - E_g)^r$$

where E_g, is the optical band gap, and 'r' is the index which has different values (2, 3, l/2 and 1/3) corresponding to indirect allowed, indirect forbidden, direct allowed and direct forbidden transitions, respectively. B is a constant called the band tailing parameter and υ is the energy of incident photons. Here the optical band gap refers to the photons assisting the electrons to move from valence band to conduction band. The optical band gap between valence band and conduction band in oxide glasses can be determined from the position of the absorption edge. The absorption edge gives information about the width of the localized states in the band gap which arises due to disorder in the glass matrix. The optical band gap energy also provides information about the nature of chemical bonds and glass structure. The typical $(\alpha h\upsilon)^{1/2}$ versus photon energy $(h\upsilon)$ [fig.4]for indirect allowed transitions, $(\alpha h\upsilon)^3$ versus $(h\upsilon)$ for direct forbidden[fig.5], $(\alpha h\upsilon)^{1/3}$ versus $(h\upsilon)$ for indirect forbidden[fig.6] and $(\alpha h\upsilon)^2$ versus $(h\upsilon)$ [fig.7] direct allowed transitions (called as Tauc's plot) have been plotted to find the values of optical band gap energy, E_g. The values of E_g are obtained by extrapolating the linear region of the curve to the (x) axis, i.e. $(\alpha h\upsilon)^{1/2}=0$ and $(\alpha h\upsilon)^2=0$ for indirect and direct transitions. The values of E_g are given in Table 1.

The value of band gap can be obtained by extrapolating the linear region of $(a/\lambda)^{1/r}$ verses (l/λ) curve at $(a/\lambda)^{1/r}=0$. The x-axis intersect value is multiplied with 1239.83, it is found that the best fit is observed for r=2. This value of band gap, designated as E_{opt}^{asf} in eV, is calculated from the parameter λ_g using the expression [1, 28]

$$E_{opt}^{asf} = \frac{1239.83}{\lambda_g}$$

The values of optical band gaps E_{opt}^{asf} of the present glass samples calculated using ASF method. It is observed that the values of optical band gap energy (E_g) match the values of optical band gap energies E_{opt}^{asf} calculated from ASF method.

3.3.2. Urbach Energy

The Urbach energy, ΔE is defined as the energy gap between localized tail states in the forbidden band gap [1]. It provides a measure of disorder in the amorphous and crystalline solids [22]. In amorphous materials, tructural disorder dominates and this could be due to the presence of structural defects like dangling bonds or non bridging oxygen atoms [23]. In borate based glass network, the higher the concentration of NBO's, the smaller is the optical band gap energy and the greater are the Urbach energy values [1, 22]. When the energy of the incident photon is less than the band gap, the increase in absorption coefficient is followed with an exponential decay of density of localized states into the gap [23] and the edge is known as the Urbach energy. The lack of crystalline long-range order in amorphous/glassy materials is associated with a tailing of density of states [24]. At lower values of the absorption coefficient (a), the extent of the exponential tail of the absorption edge characterized by the Urbach energy is given by [24]

$$\alpha = \alpha_o \exp\left(\frac{h\upsilon - E}{E_u}\right)$$

where Eu is Urbach energy

The ΔE values are evaluated from the Urbach plots [Fig.8] of ln (α) versus $(h\upsilon)$ by taking the reciprocal of the slopes of the linear portion of the curves and are listed in Table.1. The variation Urbach energy (ΔE) with CaO concentration is non- linear with increase of CaO content.

3.3.3. Refractive Index

Refractive index (n) was determined from the optical band gap energy (E_g) using the formula proposed by Dimitrov and Sakka [28, 38]

$$\frac{(n^2-1)}{(n^2+2)} = 1-\sqrt{\frac{E_{opt}^{asf}}{20}}$$

The refractive index (n) values were calculated from the above equation and are given in Table 1. The refractive index values of the present glass samples are in the range 2.423 to 2.446.

3.3.4. Molar refraction (R_m)

The product of reflection loss and molar volume is called molar refraction R_m (cm^3). This parameter is related to the structure of the glass are given by the Lorentz- Lorentz equation where R_m is directly proportional to V_m as follows [39]

$$R_m = \left(\frac{n^2-1}{n^2+2}\right) V_m$$

where "n" is the refractive index, V_m is molar volume and the term $(n^2-1)/(n^2+2)$ represents the reflection loss. The values of molar refraction R_m are presented in Table.1.

3.3.5. Molar electronic polarizability (α_m)

According to Clausios-Mosotti, the molar electronic polarizability α_m is given by the relation [39]

$$\alpha_{m=} \left(\frac{3}{4\pi Na}\right) R_m$$

where Na is Avogadro's number.
The values of molar electronic polarizability α_m are presented in Table.1.

3.3.6. Dielectric constant

The dielectric constant was calculated from the refractive index calculated from UV-Vis absorption data and from optical band gap obtained from absorption and is given by [7]

$$\varepsilon = n^2$$

Where n is refractive index.

3.3.7. Optical dielectric constant

The Optical dielectric constant is defined as square of the refractive index minus one [7] i.e.

$$\varepsilon_{o=} n^2 - 1$$

Where n is refractive index.

3.3.8. Electrical susceptibility (χ)

The electrical susceptibility (χ) was calculated by formula [7]

$$(n^2 - 1)/4\pi$$

Where n is refractive index.

3.4. Infrared spectra

 FTIR transmittance spectra (fig.9)showed fine intense absorption bands centered around 1800, 1340, 900, 690, 497 and 280 cm^{-1} and small shoulders around 270,300, 352, 1740, 2300, and 3400 cm^{-1}. The sharp intense band around 1340 cm-1 are due to symmetric stretching vibration of B-O bonds in BO_3 units varied from Pyro, Ortho borate groups respectively. A sharp band around 1338, 1344, 1336, 1315, 1313 cm^{-1} are due to B-O symmetric stretching vibration in BO_3 units from Pyro and Ortho borate groups, and these are highest intensity bands. The sharp band around 690 cm^{-1} is due to the bending vibrations of B-O-B units in BO_3 triangles. The broad intense band around 900 cm^{-1} is assigned to stretching vibrations of BO_4 units in various structural groups.2920 cm^{-1} and 3020 cm^{-1} presence of hydroxyl or water groups present in the glass. The absence of peak at 806 cm^{-1} indicates the absence of Boroxol ring in vitreous B_2O_3 glasses, 883 cm^{-1} band is due to Bi-O and /or Bi-O-Bi in [BiO_6] octahedral. The peak at 704 to 713 cm^{-1} is due to B-O-B bending in oxygen bridges between two trigonal boron atoms.

IV. FIGURES AND TABLES
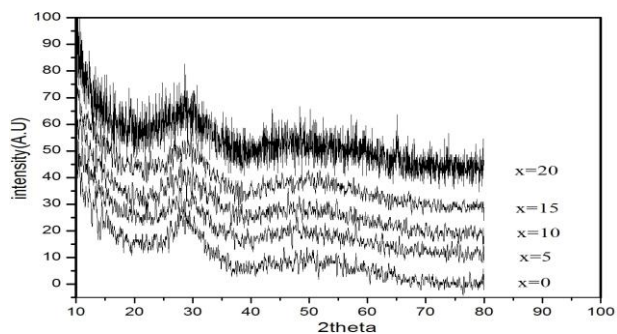
Fig.1.XRD of doped glasses
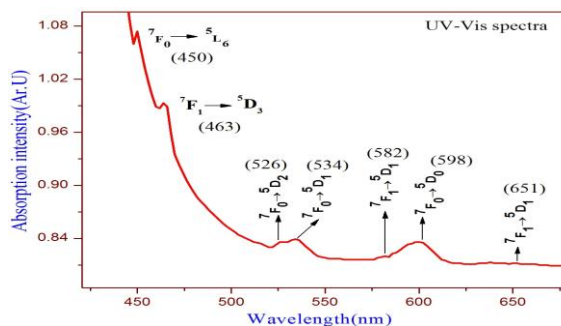
Fig.2: UV-Vis Absorption spectra
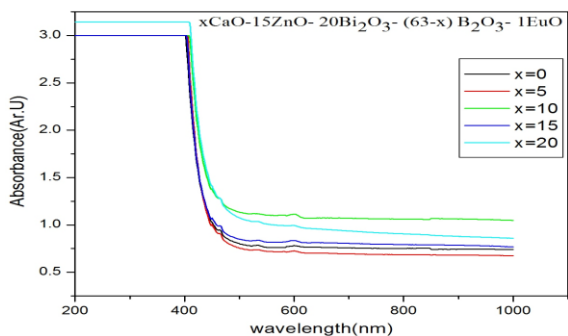
Fig.3: Cutoff wavelengths from UV graph
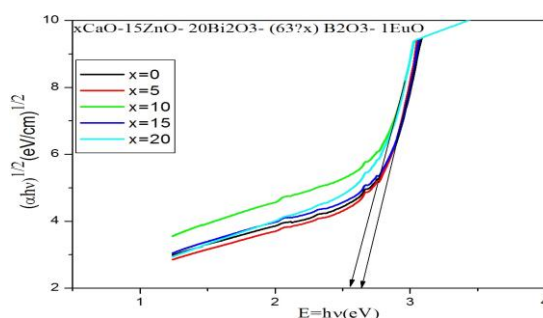
Fig.4.Tauc's plots $(\alpha h\upsilon)^{1/2}$ verses $(h\upsilon)$
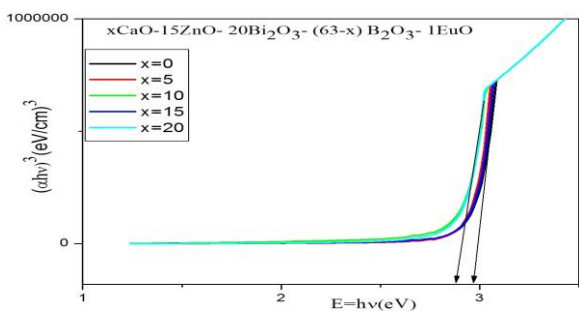
Fig.5.Tauc's plots $(\alpha h\upsilon)^{3}$ verses $(h\upsilon)$
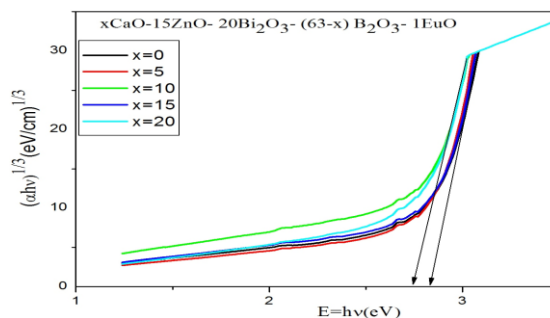
Fig.6.Tauc's plots $(\alpha h\upsilon)^{1/3}$ verses $(h\upsilon)$
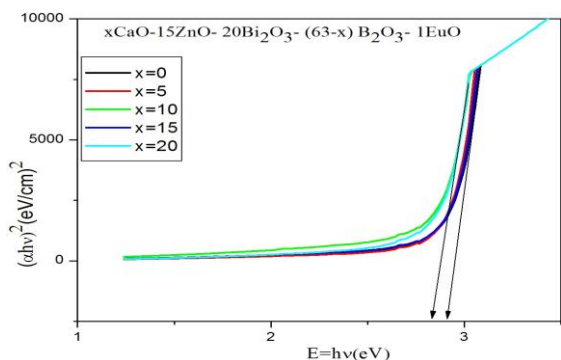
Fig.7: Tauc's plots $(\alpha h\upsilon)^{2}$ verses $(h\upsilon)$
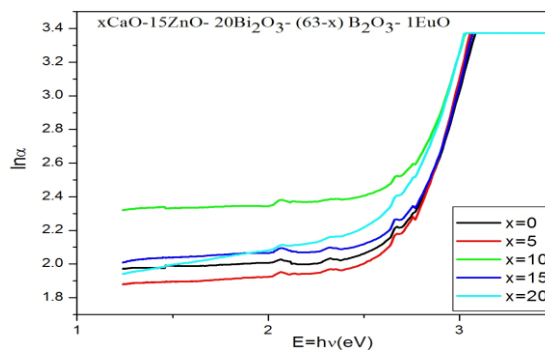
Fig.8: Urbach's plots $\ln(\alpha)$ verses $(h\upsilon)$
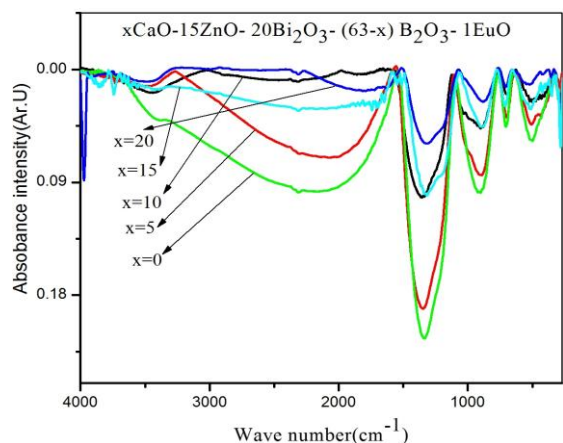
Fig.9. FTIR transmittance spectra
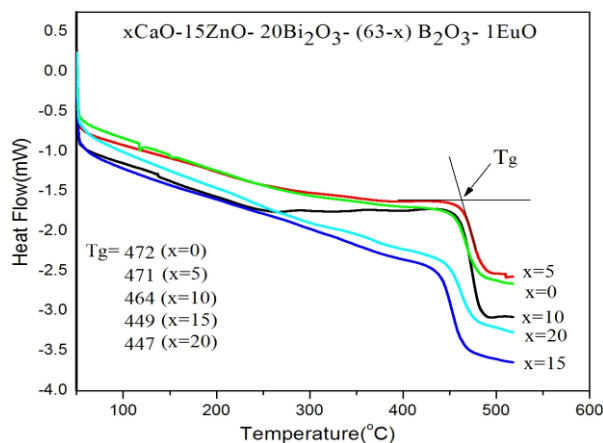
Fig.10.DSC: Temperature Vs heat flow
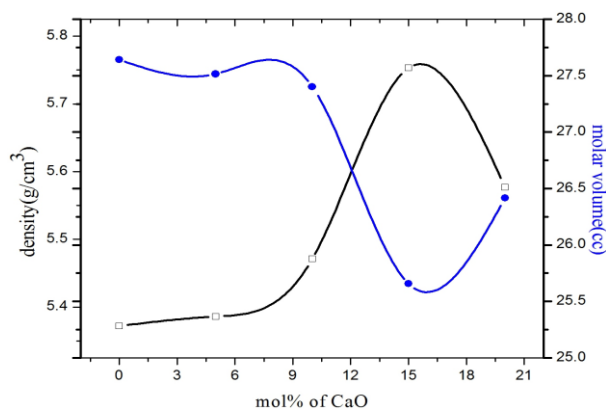
Fig.11.density, molar volume Vs mol % of CaO

Table.1: optical band gap, Cutoff wavelength, Urbach Energy, Reflection loss, Refractive index.

SN	Sample name	Cutoff wavelength	r=1/2	r=1/3	r=2	r=3	Urbach Energy	Reflection loss	Refractive index	R_m (cm^3)	α_m (10^{-24})(Å^3)	A.M.W (gm)	Tg (^{o}C)
1	ZCB0	434	2.689	2.772	2.894	2.891	0.269	0.6196	2.426	17.13	6.79	148.48	472
2	ZCB5	431	2.699	2.803	2.899	2.908	0.251	0.6193	2.425	17.04	6.76	148.2	471
3	ZCB10	434	2.645	2.704	2.826	2.829	0.301	0.6241	2.446	17.10	6.78	149.9	464
4	ZCB15	432	2.646	2.779	2.907	2.899	0.296	0.6187	2.423	15.87	6.29	147.61	449
5	ZCB20	441	2.578	2.736	2.851	2.844	0.304	0.6224	2.438	16.44	6.52	147.33	447

Table.2: Observed IR absorption band in Eu^{3+} ions doped alkaline earth oxide Zinc bismuth borate glasses.

S No	sample	IR absorption bands							
1	ZCB0	281	497	690	902	1338	1788	2318	3421
2	ZCB5	285	507	698	893	1344	------	2071	3489
3	ZCB10	270	499	704	902	1336	------	2312	3408
4	ZCB15	277	543	707	879	1313	1859	2312	3514
5	ZCB20	279	514	709	883	1315	1741	2312	3417

Table.3. Vibration types of different IR wave numbers.

Range of wave numbers (cm^{-1})	Vibration types
270-285	Zn-O vibrations in ZnO4 units [27, 36]
420–522	Bi–O–Bi stretching vibration of [BiO_6] octahedral [26, 30]
692–713	Bending vibration of BO_4 units [26, 32, 33]
881–920	Stretching vibration of [BiO_3]/ [BO_4] units [26, 35, 36]
1317–1363	Stretching vibration of B–O–B in [BO_3] triangles [26, 30, 33]
1600-1800	Bending modes of OH groups [27, 36]
2304-2380	Anti symmetric stretching of water molecule [28, 37]
2620-2920	Hydrogen bonding [28, 37]
3400-3460	O-H stretching vibration [28, 37]

Table.4: physical properties

S.No	sample	$\rho(g/cm^2)$	$V_m(cc)$	$Ni(x10^{20})$	$R_p(nm)$	$R_i(nm)$	(f) $(x10^{15}cm^{-2})$	ε	ε_o	χ
1	ZCB0	5.372	27.641	2.1786	0.0401	0.153	1.871	5.8854	4.8854	0.3888
2	ZCB5	5.386	27.515	2.1886	0.0399	0.1523	1.888	5.8806	4.8806	0.3885
3	ZCB10	5.471	27.401	2.1978	0.0397	0.1517	1.904	5.9829	4.9829	0.3966
4	ZCB15	5.753	25.657	2.34712	0.03717	0.14202	2.171	5.87093	4.87093	0.38769
5	ZCB20	5.577	26.417	2.2796	0.0383	0.1462	2.048	5.9438	4.9438	0.3935

V. CONCLUSIONS
✓ the XRD studies confirms the glassy nature of the samples prepared.

✓ The DSC plots and calculated transition temperature shows that the T_g is decreasing with increase in the content of CaO, and hence decreasing melting temperature.

✓ The FTIR studies revealed that, in the glass matrix, various borate groups are randomly interconnected typical borate groups like ortho borate glasses. From FTIR spectra it is also evident that present glasses consist of pyro, ortho BO_3 and octahedral BiO_6 structural units and with increase of CaO content the intensity of absorption peaks is decreasing (fig.10) hence we can say that these glasses are more transparent with more content of CaO.

✓ From the optical data the evaluated values of optical band gap energy (E_g) matches with the values of optical band gap energies E_{opt}^{asf} calculated from ASF method. The variation of Urbach energy (ΔE) with CaO concentration is varying non- linearly with increase of CaO contents.

REFERENCES

[1]   C.R. Kesavulu, K. Kiran Kumar, N. Vijaya, Ki-Soo Lim, C.K. Jayasankar, Materials Chemistry and Physics 141 (2013) 903e911
[2]   D. Ruter, W. Bauhofer, Appl. Phys. Lett. 69 (1996) 892.
[3]   D.A. Turnbull, S.Q. Gu, S.G. Bishop, J. Appl. Phys. 80 (1996) 2436.
[4]   P.E.A. Mobert, E. Heumann, G. Huber, B.H.T. Chai, Appl. Phys. Lett. 73(1998) 139.
[5]   S. Schweizer, L.W. Hobbs, M. Secu, J. Spaeth, A. Edgar, G.V.M. Williams, Appl.Phys. Lett. 83 (2003) 449.
[6]   T. Tsuboi, Eur. Phys. J. Appl. Phys. 26 (2004) 95.
[7]   Xavier Joseph, Rani George, Sunil Thomas, Manju Gopinath, M.S. Sajna, N.V. Unnikrishnan, Optical Materials 37 (2014) 552–560
[8]   X. Feng, S. Tanabe, T. Hanada, J. Am. Ceram. Soc. 84 (2000) 165.
[9]   S.E. Stokowski, M.E. Martin, S.M. Yarema, J. Non-Cryst. Solids 40 (1980) 481.
[10]   C.B. Layne, M.J. Weber, Phys. Rev. B 16 (1977) 3259.
[11].   C.H. Kam, S. Buddhudu, Journal of Quantitative Spectroscopy &Radiative Transfer 87 (2004) 325–337
[12].   V. Venkatramu, P. Babu, C.K. Jayasankar, Spectrochimica Acta Part A 63 (2006) 276–281
[13]   K. Swapna, Sk.Mahamuda, A.SrinivasaRao, T.Sasikala, P.Packiyaraj, L.RamaMoorthy, G.VijayaPrakash, Journal of Luminescence156(2014)80–86
[14]   T. Chengaiah, B.C. Jamalaiah, L. Rama Moorthy, Spectrochimica Acta Part A: Molecular and Biomolecular Spectroscopy 133 (2014) 495–500
[15]   J.M. Parka, H.J. Kima, Sunghwan Kim, P. Limsuwan, J. Kaewkhao Procedia Engineering 32 (2012) 855 – 861
[16]   S. Surendra Babua, P. Babu, C.K. Jayasankar, W. Sievers, Th. Tro ster, G. Wortmann, Journal of Luminescence 126 (2007) 109–120
[17]   K. Upendra Kumar, S. Surendra Babu, Ch. Srinivasa Rao, C.K. Jayasankar, Optics Communications 284 (2011) 2909–2914
[18]   K. Linganna, C.K. Jayasankar, Spectro chimica Acta Part A: Molecular and Biomolecular Spectroscopy 97 (2012) 788–797
[19]   P. Babu, C.K. Jayasankar Physica B. 279 (2000) 262-281
[20]   D. Ramachari, L.RamaMoorthy, C.K.Jayasankar, Journal ofLuminescence143(2013)674–679
[21]   M. Murali Mohan, L. Rama Moorthy, D. Ramachari, C.K. Jayasankar, Spectrochimica Acta Part A: Molecular and Biomolecular Spectroscopy 118 (2014) 966–971
[22]   F. Urbach, Phys. Rev. 92 (1953) 1324.
[23]   B. Abay, H.S. Gudur, Y.K. Yogurtchu, Solid State Commun. 112 (1999) 489.
[24]   M.A. Hassan, C.A. Hogarth, J. Mater. Sci. 23 (1988) 2500.
[25]   M. Mirzayi, M.H. Hekmatshoar, Ionics 15 (2009) 121.
[26]   I. Pal, A. Agarwal, S. Sanghi, M.P. Aggarwal, Optical Materials 34 (2012) 1171–1180
[27]   Joao Coelho, Cristina Freire, N. Sooraj Hussain, Spectrochimica Acta Part A 86 (2012) 392– 398
[28]   D. Rajesh, Y.C.Ratnakaram, M.Seshadri, A.Balakrishna, T.SatyaKrishna, Journal of Luminescence 132 (2012) 841–849
[29]   I. Arul Rayappan, K.Selvaraju, K.Marimuthu Physica B 406 (2011) 548–555
[30]   S.G. Motka, S.P. Yawale, S.S. Yawale, Bull. Mater. Sci. 25 (2002) 75.
[31]   M.E. Lines, A.E. Miller, K. Nassau, K.B. Lyons, J. Non-Cryst. Solids 89 (1987)163.
[32]   R. Iordanova, V. Dimitrov, Y. Dimitriev, D. Klissurski, J. Non-Cryst. Solids 180(1994) 58.
[33]   E.I. Kamitsos, A.P. Patsis, M.A. Karakassides, G.D. Chryssikos, J. Non-Cryst.Solids 126 (1990) 52.
[34]   A.K. Hassan, L. Borjesson, L.M. Torell, J. Non-Cryst. Solids 172–174 (1994) 154.
[35]   G. El-Damrawi, K. El-Egili, Physica B 299 (2001) 180.
[36]   S.S. Das, B.P. Baranwal, P. Singh, V. Srivastava, Infrared spectroscopic studies of ion-conducting silver phosphate glasses doped with   zinc and cadmium halides,Prog. Cryst. Growth Charact. Mater. 45 (2002) 89–96.
[37]   Cristiane N. Santos, Domingos De Sousa Meneses, Partick Echegut, Daniel R. Neuville, Antonio C. Hernandes, Alain Ibanez, Appl. Phys. Lett. 94 (2009) 151901.
[38]   V. Dimitrov and S. Sakka, I, Journal of Applied Physics, vol. 79, no. 3, pp. 1736–1740, 1996.
[39]   K Chandra Sekhar, Abdul Hameed, G. Ramadevudu, M. Narsimha Chary and Md. Shareefuddin, Proceedings of the 2nd National Conference on Applied Physics and Materials Science, Vasai College of Engineering, Hyderabad, A.P. 1-2 August, 2014. pp.113-l16.